

***Ab Initio* Finite-Temperature Excitons**Andrea Marini<sup>1</sup><sup>1</sup>*European Theoretical Spectroscopy Facility (ETSF), CNR-INFM Institute for Statistical Mechanics and Complexity, CNISM and Dipartimento di Fisica, Università di Roma "Tor Vergata," via della Ricerca Scientifica 1, I-00133 Roma, Italy*  
(Received 20 December 2007; revised manuscript received 24 July 2008; published 4 September 2008)

The coupling with the lattice vibrations is shown to drastically modify the state-of-the-art picture of the excitonic states based on a frozen-atom approximation. The zero-point vibrations renormalize the bare energies and optical strengths. Excitons acquire a nonradiative lifetime that decreases with increasing temperature. The optical brightness turns out to be strongly temperature-dependent such as to induce bright to dark (and vice versa) transitions. The finite-temperature experimental optical absorption spectra of bulk Si and hexagonal BN are successfully explained without using any external parameter.

DOI: [10.1103/PhysRevLett.101.106405](https://doi.org/10.1103/PhysRevLett.101.106405)

PACS numbers: 71.35.Cc, 65.40.-b, 71.38.-k

The *ab initio* description of the excitonic states, obtained by solving the Bethe-Salpeter (BS) equation of the many-body perturbation theory, constitutes a well-established approach to interpret the photoexcited properties of bulk materials, surfaces, nanostructures, and organic or biomolecules [1]. Although absorption and photoluminescence experiments are usually performed at room temperature, in the standard approach the BS equation is solved assuming the atoms frozen in their crystallographic positions, thus neglecting the effect of lattice vibrations. As a consequence, excitons turn out to be insensitive to the temperature  $T$  and to have an infinite lifetime. This is in stark contrast with the experimental results, where the absorption and emission lines at *any* temperature show an intrinsic width that reflects the *finite* lifetime of the underlying excitonic states. Moreover, in bulk semiconductors, it is a well-known fact that the absorption line position, width, and intensity show a clear  $T$  dependence [2]. In the frozen-atom BS equation, this dependence is not described at all. Even in the  $T \rightarrow 0$  limit, where atoms vibrate to fulfill the uncertainty principle (zero-point vibrations), the calculated absorption spectra is commonly convoluted with some artificial, *ad hoc* numerical broadening function chosen to yield the best agreement with the experiment. More generally, the finite-temperature properties of the excitons define their quantum efficiency as photoemitters, a key parameter in devising materials for optoelectronic applications.

Bulk silicon (Si) and hexagonal boron nitride (*h*-BN) are two paradigmatic semiconductors whose optical properties show remarkable differences. Si is one of the most deeply investigated material in the *ab initio* community [1]. Although its optical properties have been studied in different theoretical frameworks [1], the finite-temperature dielectric function, measured by Lautenschlager and Jellison [3] twenty years ago, remains still unexplained. While Si has a small indirect gap, *h*-BN is a wide direct gap quasi-two-dimensional semiconductor [4]. At difference with Si, *h*-BN optical spectra are dominated by a bound exciton

with a large binding energy ( $\sim 0.7$  eV). Very recent results by Watanabe, Taniguchi, and Kanda [5] stimulated interest in this material for possible applications as an ultraviolet laser device.

In this Letter, I solve, in a fully *ab initio* manner, the Bethe-Salpeter equation including the coupling with the lattice vibrations. The picture of the excitons obtained within a frozen-atom approximation turns out to be deeply modified, both at zero and finite temperature. Excitons acquire a nonradiative lifetime, otherwise infinite in the frozen-atom approximation. The finite-temperature optical spectra of Si and *h*-BN are reproduced in excellent agreement with the experimental results. The thermal properties of the excitonic states are explained in terms of a weak (Si) and a strong (*h*-BN) exciton-phonon coupling. In Si, the lattice vibrations affect only the electron-hole substrate of the excitonic states, while in *h*-BN, they participate actively in the exciton buildup. In *h*-BN, this strong coupling induces bright to dark (and vice versa) transitions and reduces, at zero temperature, the lowest exciton binding energy by  $\sim 30\%$ .

In the frozen-atom (FA) BS equation, the excitonic states  $|\lambda_{\text{FA}}\rangle$  and energies  $E_{\lambda}^{\text{FA}}$  are eigenstates and eigenvalues of the Hamiltonian  $\mathbf{H}^{\text{FA}}$ , written in the electron ( $e$ ) hole ( $h$ ) basis [1]

$$H_{ee',hh'}^{\text{FA}} = (E_e - E_h)\delta_{eh,e'h'} + (f_e - f_h)\Xi_{ee',hh'}, \quad (1)$$

with  $E_{e(h)}$  and  $f_{e(h)}$  the quasielectron (hole) energies and occupations.  $\Xi$  is the Bethe-Salpeter kernel that is a sum of a direct and an exchange electron-hole ( $e$ - $h$ ) scattering:  $\Xi_{ee',hh'} = \langle eh|W - 2V|e'h'\rangle$ .  $W$  is the statically screened and  $V$  is the bare Coulomb interaction. The absorption spectrum is given by the imaginary part of the dielectric function  $\epsilon_2(\omega) = -(8\pi/V)\sum_{\lambda}|S_{\lambda}^{\text{FA}}|^2\text{Im}[(\omega - E_{\lambda}^{\text{FA}} + i\eta)^{-1}]$ , where  $S_{\lambda}^{\text{FA}} = \langle GS|i\hat{\xi} \cdot \vec{r}|\lambda_{\text{FA}}\rangle$  are the excitonic optical strengths,  $\eta$  is a broadening parameter,  $V$  is the crystal volume, and  $\hat{\xi}$  is the light polarization direction. Equation (1) is *ab initio* because the single-particle ener-

gies and the kernel  $\Xi$  are calculated starting from density-functional theory (DFT) wave functions and energies, with no adjustable parameters [6]. In the standard approach, the quasiparticle (QP) energies  $E_{e,h}$ , obtained within the GW approximation for the electronic self-energy [1], are assumed to be real and independent on  $T$ . This approximation is justified by the fact that the smallest excitation energy in a semiconductor, the gap energy  $E_g$ , is usually much larger than the thermal energy corresponding to typical experimental temperatures, i.e.,  $T \ll E_g/k_b$ . The Hamiltonian  $\mathbf{H}^{\text{FA}}$  is then Hermitian [1] and  $T$  independent. As a consequence, the energies  $E_\lambda^{\text{FA}}$  are real, and  $\eta$  is used as an *a posteriori* parameter to mimic the experimental broadening of the absorption peaks [7].

In the finite-temperature regime, the levels  $E_i$  acquire an explicit dependence on the temperature:  $E_i(T) = E_i + \Delta E_i(T)$ , with  $\Delta E_i(T) = \Delta E_i^{e\text{-ph}}(T) + \Delta E_i^{\text{TE}}(T)$ .  $\Delta E^{\text{TE}}$  is the thermal expansion (TE) contribution [2,8].  $\Delta E^{e\text{-ph}}$  represents the *complex* energy correction that arises from the electron-phonon (*e-ph*) interaction. In this work, the *e-ph* interaction is treated in the Heine, Allen, and Cardona approach [2] where  $\Delta E^{e\text{-ph}}$  can be rewritten in terms of an *e-ph* coupling function  $g^2 F_i(\omega)$ :

$$\Delta E_i^{e\text{-ph}}(T) = \int d\omega g^2 F_i(\omega) [N(\omega, T) + 1/2], \quad (2)$$

with  $N(\omega, T) = (e^{\beta\omega} - 1)^{-1}$  being the Bose occupation function. The complex  $g^2 F_i$  function is given by

$$g^2 F_i(\omega) = \sum_\nu \frac{\partial E_i}{\partial N(\omega_\nu, T)} \delta(\omega - \omega_\nu), \quad (3)$$

with the sum is extended to all phonon modes  $\nu$  [9]. Equations (2) and (3) tell that  $\text{Re}[\Delta E_i^{e\text{-ph}}]$  arises from the quadratic contribution to the expansion of  $E_i(T) - E_i$  in the atomic displacements. As shown in Ref. [11], the QP states can also decay emitting phonons, thus acquiring a finite lifetime ( $\propto 1/\text{Im}[\Delta E_i^{e\text{-ph}}]$ ).

The temperature dependence of the QP states, arising from the *e-ph* interaction, modifies Eq. (1) [12]. As the  $E_{e,h}(T)$  functions are complex, the BS Hamiltonian turns in a *non-Hermitian* operator

$$H_{hh'}^{ee'}(T) = H_{hh'}^{\text{FA}} + [\Delta E_e(T) - \Delta E_h(T)] \delta_{eh,e'h'}, \quad (4)$$

and the excitonic states are the solution of the eigenproblem  $H(T)|\lambda(T)\rangle = E_\lambda(T)|\lambda(T)\rangle$ . The eigenstates  $|\lambda(T)\rangle$  are linear combinations of *e-h* pairs:  $|\lambda(T)\rangle = \sum_{eh} A_{eh}^\lambda(T) |eh\rangle$ , with  $A_{eh}^\lambda = \langle eh|\lambda\rangle$ . If we plug this expansion into the definition of the excitonic energies  $E_\lambda(T) = \langle \lambda(T)|\mathbf{H}|\lambda(T)\rangle$ , we get

$$E_\lambda(T) = \langle \lambda(T)|\mathbf{H}^{\text{FA}}|\lambda(T)\rangle + \sum_{eh} |A_{eh}^\lambda(T)|^2 [\Delta E_e(T) - \Delta E_h(T)]. \quad (5)$$

Using Eq. (2) and neglecting the TE term, Eq. (5) yields

$$\begin{aligned} \text{Re}[\Delta E_\lambda(T)] &= [\langle \lambda(T)|\mathbf{H}^{\text{FA}}|\lambda(T)\rangle - \langle \lambda_{\text{FA}}|\mathbf{H}^{\text{FA}}|\lambda_{\text{FA}}\rangle] \\ &+ \int d\omega \text{Re}[g^2 F_\lambda(\omega, T)] [N(\omega, T) + 1/2], \end{aligned} \quad (6)$$

$$\text{Im}[E_\lambda(T)] = \int d\omega \text{Im}[g^2 F_\lambda(\omega, T)] [N(\omega, T) + 1/2], \quad (7)$$

where  $\Delta E_\lambda(T) = E_\lambda(T) - E_\lambda^{\text{FA}}$  and I have introduced the exciton-phonon coupling function  $g^2 F_\lambda(\omega, T) = \sum_{eh} |A_{eh}^\lambda(T)|^2 [g^2 F_e(\omega) - g^2 F_h(\omega)]$ . Equations (6) and (7) constitute a key result of this work. Equation (7) defines, in an *ab initio* manner, the nonradiative excitonic lifetime  $\tau_{\text{nr}}^\lambda = \{2\text{Im}[E_\lambda(T)]\}^{-1}$  that is otherwise infinite in the FA approximation. The dielectric function now depends explicitly on  $T$ :  $\epsilon_2(\omega, T) = -(8\pi/V) \sum_\lambda |S_\lambda(T)|^2 \text{Im}\{[\omega - E_\lambda(T)]^{-1}\}$ , and no damping parameter  $\eta$  is needed anymore.

Equation (6) defines the temperature dependence of the excitonic energies and is composed of two contributions: The integral of the  $g^2 F_\lambda$  function arises from the renormalization of the electron-hole pairs  $|eh\rangle$  that constitute the excitonic packet (with amplitudes  $A_{eh}^\lambda$ ). This term represents an *incoherent contribution*, where the electrons and holes interact separately with the lattice vibrations. The first term, instead, describes an active participation of the phonon modes in the excitonic state buildup. It is, then, a *coherent* contribution that modifies the  $A_{eh}^\lambda$  components and vanishes when  $|\lambda(T)\rangle = |\lambda_{\text{FA}}\rangle$ . Thus Eqs. (6) and (7) define two physical regimes of the exciton-phonon interaction: In the *weak coupling* case,  $|\lambda(T)\rangle \approx |\lambda_{\text{FA}}\rangle$ , and the incoherent contribution is dominant (this is the case of Si). *h-BN*, instead, belongs to the *strong coupling* case, where the coherent term in Eq. (6) cannot be neglected.

A remarkable property of Eqs. (6) and (7) is that, although  $N(\omega, T \rightarrow 0) = 0$ , the excitonic energies do not reduce to the FA values and the excitonic lifetimes remain finite when  $T \rightarrow 0$ , because of the 1/2 factor. This factor arises from the quantum-mechanical vibrations of the atoms when  $T = 0$  (the so-called zero-point vibrations [13]).

The experimental finite-temperature optical spectra of Si [3], shown in Fig. 1, are dominated by two excitonic peaks ( $E_1$  and  $E_2$ ) resonant with the electron-hole continuum and characterized by a moderate *e-h* attraction. As the temperature increases, the  $E_{1,2}$  peaks move towards lower energies, with a width that increases with  $T$ . This gradual redshift has been studied only in an independent-particle approximation (IPA) [11], thus neglecting excitonic effects. While the IPA shows only a weak dependence on  $T$ , both the peak position and widths of the  $E_{1,2}$  peaks are well reproduced by the results of the finite- $T$  BS equation,

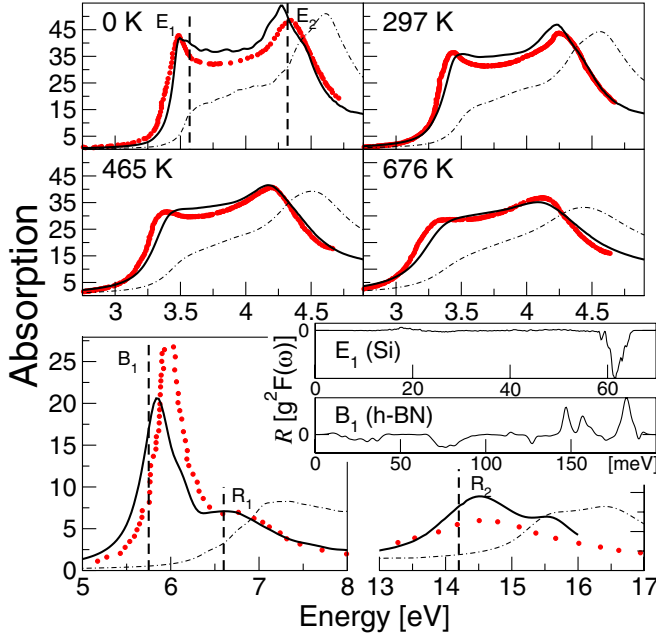


FIG. 1 (color online). Optical absorption of bulk Si (upper frames) for several temperatures and of *h*-BN (lower frames) at room temperature. The experimental spectra [3,15] (circles) are compared with the BS equation (solid line) and with the independent-particle approximation (dotted-dashed line). In the insets, the exciton-phonon spectral functions  $\text{Re}[g^2 F_\lambda(\omega, T=0)]$  are shown for the  $E_1$  (Si) and  $B_1$  (*h*-BN) peaks (see text). The width of the absorption peaks reflects the damping of the excitons due to the scattering with phonons. No additional numerical damping is included. The excitonic energies obtained within the frozen-atom BS equation (represented by the vertical dashed lines) are redshifted in Si and blueshifted in *h*-BN.

shown in Fig. 1. Excitons acquire a finite damping that, starting from  $\sim 30$  meV at  $T = 0$  K and increasing to  $\sim 60$  meV at room temperature and  $\sim 150$  meV at  $T = 676$  K, is in excellent agreement with the experimental estimations [11]. Compared with the frozen-atom BS equation, the position of the  $E_1$  and  $E_2$  peaks at  $T = 0$  is redshifted by 80 meV, to correct the deviation of previous calculations from the experimental spectrum [7].

The  $g^2 F_\lambda$  function can be now used to pin down the phonon modes that contribute to the redshift of the  $E_{1,2}$  peaks. In the inset in Fig. 1, the  $\text{Re}[g^2 F_\lambda(\omega)]$  for the  $E_1$  state shows that the exciton is mainly coupled with the optical phonons (60 meV peak), with the acoustic branches giving only a small correction. As the temperature increases, the phonon population  $N$  in Eqs. (6) and (7) also increases, thus enhancing the redshift and the width of the optical peaks and leading to a linear scaling with the temperature when  $T \geq 200$  K and  $N(\omega, T) \sim 1/\beta T$ . A more careful analysis of the different contributions to  $\Delta E_\lambda(T)$  given by Eq. (6) shows that the incoherent contribution [second term in the right-hand side of Eq. (6)] is dominant. This is due to the fact that the moderate *e-h* attraction prevents the  $E_{1,2}$  excitons to behave as a unique,

bosoniclike, particles. Consequently, the lattice vibrations mainly couple with the *e-h* substrate of the excitons. It is important to note that, in this case, Eqs. (6) and (7) can be simplified using the result of the FA BS equation, as  $\Delta E_\lambda(T) \approx \int d\omega \text{Im}[g^2 F_\lambda(\omega)][N(\omega, T) + 1/2]$ , with  $|\lambda(T)\rangle \approx |\lambda_{\text{FA}}\rangle$ .

*h*-BN is an anisotropic, insulating compound, consisting of graphitelike sheets with a hexagonal structure arranged in an *ABAB*... stacking [4]. The optical and electronic properties as well as the lattice dynamics [14] are strongly influenced by the layered structure. The in-plane experimental optical absorption spectrum measured at room temperature [15] is shown in Fig. 1, lower frames. Three prominent peaks are clearly distinguishable: a bound state  $B_1$  at 5.98 eV and two resonant states  $R_1$  at 6.87 eV and  $R_2$  at 14.7 eV. The frozen-atom BS equation predicts the three peak energies to be 5.75, 6.6, and 14.2 eV [16] and 0.1–0.5 eV redshifted if compared to the experiment.

The room-temperature solution of the BS equation is compared with the experiment in Fig. 1. Both experimental peak positions and widths are well described, and the  $B_1$ ,  $R_1$ , and  $R_2$  states are blueshifted by 0.07, 0.17, and 0.3 eV compared to the frozen-atom BS equation results. The different sign of the phonon-induced corrections of the excitonic peak positions is the first striking difference with the case of Si and can be understood by looking at the function  $\text{Re}[g^2 F_\lambda(\omega)]$  for the  $B_1$  state, shown in the inset in Fig. 1. The anisotropic structure of *h*-BN is reflected in the rich series of phonon peaks in the  $g^2 F_\lambda$  function. The phonon modes corresponding to the peaks at  $\sim 30$  and  $\sim 75$  meV are polarized perpendicularly to the hexagonal layers [14]. As the bound excitons are spatially confined within the layer [16], these modes tend to stretch the layers, thus increasing the exciton localization and, consequently, its binding energy. The high-energy modes ( $\omega \geq 100$  meV), instead, are polarized parallel to the layer. These modes correspond to in-plane vibrations that interfere with the binding of the *e-h* pairs embodied in the excitonic state, counteracting the excitonic localization. Their stronger positive contribution to the  $g^2 F_\lambda$  function causes an overall blueshift of the absorption peaks and a reduction of the exciton binding energy. Similarly to the case of Si, the *h*-BN QP optical gap is shrank by the electron-phonon coupling by 0.12 eV. Thus we get an overall reduction of the lowest exciton binding energy of 0.2 eV that is 30% of the value obtained by neglecting the exciton-phonon coupling (0.72 eV).

The thermal evolution of the excitonic energies and optical strengths  $|S_\lambda(T)|^2$  for the near-gap excitons is shown in Fig. 2. The size of the circles is proportional to  $|S_\lambda|^2$ . The opposite contribution to the  $g^2 F_\lambda$  function of the low- and high-energy phonons makes the excitonic energies almost constant for  $T \leq 500$  K, in agreement with the experimental observation [17]. In contrast, the excitonic optical strength drastically depends on the temperature. We

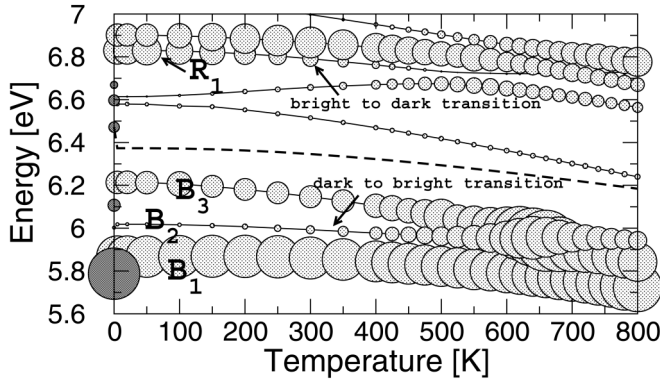


FIG. 2. Temperature dependence of the energies and oscillator strengths of the near-gap excitons (bound and resonant) in  $h$ -BN. The dashed line indicates the energy position of the optical gap in the independent-particle approximation. The sizes of the circles are proportional to the excitonic optical strength. The darker circles at  $T = 0$  is the result obtained neglecting exciton-phonon coupling. At  $T = 0$  we observe a 30% reduction of the  $B_1$  exciton binding energy due to the zero-point lattice vibrations. The  $B_2$  and  $R_1$  excitons, instead, undergo a bright to dark (and vice versa) transition at room temperature (see text).

see that the  $R_1$  (resonant) and the  $B_2$  (bound) excitons undergo a bright to dark (and vice versa) transition at room temperature. Indeed, we have that  $S_\lambda(T) - S_\lambda^{\text{FA}} = \langle GS | e^{i\hat{\xi} \cdot \vec{r}} [|\lambda(T)\rangle - |\lambda_{\text{FA}}\rangle] \rangle$ , so that this astonishing effect is entirely due to the coherent contribution  $\Delta[E_\lambda(T)]$ , given by the first term in Eq. (6).

From Fig. 2, we notice that the  $B_2$  and  $R_1$  transitions occur only when a bundle of states get close in energy. The  $B_2$  state, for example, acquires optical strength only when it approaches the  $B_3$  state. The microscopical mechanism of the bright to dark (and vice versa) transitions is, then, a transfer of optical strength between energetically close excitonic states. In the case of the  $B_2$  exciton, for example, this process occurs by means of a mixing with the  $B_3$  state that induces an increase of the contribution from bands with different parity in the  $e$ - $h$  pairs embodied in the  $B_2$  state. This induces a finite dipole and a finite absorption cross section. In the case of resonant excitons (with energy larger than the optical gap  $E_g$ ), this hybridization is possible because of the continuum  $e$ - $h$  substrate which connects the states. However, the bound excitons are discrete states, and the  $e$ - $h$  substrate is replaced by the energy indetermination due to the finite damping. This is confirmed by a calculation of the  $h$ -BN excitons done neglecting the exciton damping, imposing the  $E_\lambda(T)$  to be real. In this case the three bound states  $B_{1,2,3}$  energies  $E_\lambda(T)$  never cross, and the  $B_2$  state remains dark at all temperatures.

In conclusion, the electron-phonon coupling induces a severe modification of the frozen-atom picture of the excitonic states both at zero and at finite temperatures. The proposed finite-temperature Bethe-Salpeter equation de-

scribes, in a fully *ab initio* manner, a wealth of new physical features and makes clear that a proper and accurate description of the excitonic states in semiconductors and insulators cannot disregard the coupling with the lattice vibrations.

The author thanks X. Gonze, M. Cardona, and L. Wirtz for fruitful discussions and C. Hogan for a critical reading. I acknowledge support by the European Network of Excellence NQ (NMP4-CT-2004-500198).

- [1] For a review, see G. Onida, L. Reining, and A. Rubio, *Rev. Mod. Phys.* **74**, 601 (2002).
- [2] For a review, see M. Cardona, *Solid State Commun.* **133**, 3 (2005).
- [3] P. Lautenschlager, M. Garriga, L. Viña, and M. Cardona, *Phys. Rev. B* **36**, 4821 (1987); G. E. Jellison, Jr. and F. A. Modine, *ibid.* **27**, 7466 (1983).
- [4] Yong-Nian Xu and W. Y. Ching, *Phys. Rev. B* **44**, 7787 (1991).
- [5] K. Watanabe, T. Taniguchi, and H. Kanda, *Nature Mater.* **3**, 404 (2004).
- [6] DFT calculations are performed in the local density approximation (LDA) using a plane-wave basis. Excitonic and QP (in the case of  $h$ -BN) calculations have been done using the YAMBO code: <http://www.yambo-code.org>. Si QP corrections have been taken from M. S. Hybertsen and S. G. Louie, *Phys. Rev. B* **34**, 5390 (1986).
- [7] M. Cardona, L. F. Lastras-Martínez, and D. E. Aspnes, *Phys. Rev. Lett.* **83**, 3970 (1999).
- [8] W. Paszkowicz, J. B. Pelka, M. Knapp, T. Szyszko and S. Podsiadlo, *Appl. Phys. A* **75**, 431 (2002).
- [9] The  $\frac{\partial E_\lambda}{\partial N}$  factors and the phonon frequencies used to evaluate  $\Delta E^{e-ph}$  were calculated *ab initio* using the density-functional perturbation theory in the LDA approximation [10].
- [10] S. Baroni, S. de Gironcoli, A. Dal Corso, and P. Giannozzi, *Rev. Mod. Phys.* **73**, 515 (2001); PWscf project, <http://www.pwscf.org/>.
- [11] P. Lautenschlager, P. B. Allen, and M. Cardona, *Phys. Rev. B* **31**, 2163 (1985); **33**, 5501 (1986).
- [12] The coupling with the nuclear vibrations causes an additional scattering of the  $|eh\rangle$  pairs with the phonon modes that modifies the BS kernel. However, this correction is negligible for the systems considered in this work.
- [13] As shown by L. F. Lastras-Martínez *et al.*, *Phys. Rev. B* **61**, 12946 (2000), the isotope effect can be used to measure the zero-point renormalization of the dielectric function.
- [14] J. Serrano, A. Bosak, R. Arenal, M. Krisch, K. Watanabe, T. Taniguchi, H. Kanda, A. Rubio, and L. Wirtz, *Phys. Rev. Lett.* **98**, 095503 (2007).
- [15] C. Tarrio and S. E. Schnatterly, *Phys. Rev. B* **40**, 7852 (1989).
- [16] B. Arnaud, S. Lebègue, P. Rabiller, and M. Alouani, *Phys. Rev. Lett.* **96**, 026402 (2006).
- [17] M. G. Silly, P. Jaffrennou, J. Barjon, J.-S. Lauret, F. Ducastelle, A. Loiseau, E. Obraztsova, B. Attal-Tretout, and E. Rosencher, *Phys. Rev. B* **75**, 085205 (2007).